Respuestas, 25 (3), September - December 2020, pp. 250-261, ISSN 0122-820X - E ISSN: 2422-5053

Respuestas
Journal of Engineering Sciences
RESPUESTAS

Original Article
https://doi.org/10.22463/0122820X.2108

Electronic localization in Hexagonal Core-Shell Nanowires Under External Fields

Localización Electrónica en Nanohilos Hexagonales con Estructura Núcleo-Corteza en Presencia de Campos Externos

Angie Nicole Hernández Durán[1], Willian Gutiérrez Niño[2], David Alejandro Miranda Mercado[3*]

[1] *Physicist, angie-hernandez4@correo.uis.edu.co, ORCID: 0000-0001-9391-7157, Universidad Industrial de Santander, Bucaramanga, Colombia.*
[2] *Doctorate in Natural Sciences Physics, willigut@uis.edu.co, ORCID: 0000-0002-9919-7514, Universidad Industrial de Santander, Bucaramanga, Colombia.*
[3*] *PhD in Applied Chemistry, dalemir@uis.edu.co, ORCID: 0000-0003-3130-3314, Universidad Industrial de Santander, Bucaramanga, Colombia.*

Cómo citar: A. N. Hernández-Durán, W. Gutiérrez-Niño, D. A. Miranda-Mercado, "Electronic localization in Hexagonal Core-Shell Nanowires Under External Fields", *Respuestas*, vol. 25, no. 3, 250-261, 2020.

Received on March 8, 2020 - Approved on July 24, 2020.

ABSTRACT

In the framework of the free electron inside a semiconductor, we, numerically, analyzed the energy spectrum and electronic density of a GaAs-InAs Core-Shell Nanowire with hexagonal cross-section for a single electron. The effect of a magnetic field applied in the direction of growth of the structure was also considered, and the corresponding Schrödinger equation for the localization probability in the transverse plane of the structure, in the presence of the field, was solved using the software COMSOL Multiphysics®. The results allow the identification of energy shells, each composed by six levels, as a consequence of the hexagonal geometry, where six potential wells are created by the abrupt change of direction in the borders of the structure. Additionally, the Aharonov-Bohm oscillations of the system are analyzed for a structure with significant shell thickness.

Keywords:
Aharonov-Bohm oscillations, Artificial molecules, Core-Shell Nanowires, Electronic density.

RESUMEN

A partir de la aproximación de electrón libre dentro de un semiconductor, se realizó análisis numérico del espectro energético y la densidad de probabilidad electrónica de un electrón dentro de un nanohilo hexagonal con estructura núcleo-corteza. En el análisis se consideró el efecto de aplicar un campo magnético en la dirección de crecimiento del nanohilo y se resolvió numéricamente la ecuación de Schrödinger para el electrón localizado en el plano transversal de la estructura en presencia del campo externo; los cálculos se realizaron por medio de elementos finitos implementados con COMSOL Multiphysics®. Los resultados obtenidos permitieron identificar capas energéticas, compuestas, cada una, de seis niveles. Estas capas se atribuyen a la geometría hexagonal conformada por seis pozos de potencial creados por el abrupto cambio de dirección de los bordes de la estructura. Adicionalmente, se observaron las oscilaciones Aharonov-Bohm del sistema para una estructura con grosor significativo de la corteza.

Palabras clave:
Densidad de probabilidad electrónica, Moléculas artificiales, Nanohilo con estructura núcleo-corteza, Oscilaciones Aharonov-Bohm.

***Corresponding author.**
E-mail address: dalemir@uis.edu.co (David Alejandro Miranda Mercado)

Introduction

The growing interest in semiconductor nanowires (NWs), due to their Transport properties of optical and electronic excitations [1], [2], has led to diverse and increasingly specialized studies, both theoretical and experimental. The study of NWs allows to broaden the understanding and refine the control over their spectral properties, in order to achieve their practical implementation in many branches of industry, from food [3] and biomedicine [4] to satellite technology devices [5], among others.

Since the first NW obtained in 1987 at Bell Laboratories, the interest in the morphological possibilities of these structures, through the use of different fabrication techniques and different materials, resulted in the creation, in 1997, of the first core-shell nanowires (CSNWs). A CSNW consists of a NW accompanied by coaxial shells, or nanotubes (NT), of different semiconductor materials. However, it was not until 2002 that the eagerness for the characterization of these nanostructures became evident, since the different configurations of CSNWs present advantages with respect to the NW without a shell; among these advantages are the increase in photonic absorption efficiency [6], [7], spontaneous emission [8], [9], exciton surface emission [10], capacitance and electrical conductivity [11], improvement in spin-orbit coupling [12], and decrease in other properties, such as thermal conductivity [13].

The synthesis of CSNW starts with the growth of the core, i.e., a NW, usually fabricated by vapor deposition techniques. The NW serves as a support for the shell and its geometry depends on the constituent elements, e.g., fabrication of GaAs NWs results in hexagonal cross-section nanostructures, due to the crystal structure of GaAs. The geometry of the shell is determined by the cross-sectional shape of the NW; such a shell can be obtained by pyrolysis on the lateral surfaces of the NW. In particular, the growth of InAs shell on GaAs is a non-homogeneous process, because it starts with the formation of islands on the surface; however, these islands eventually widen until they merge together and form a single layer that begins to increase in thickness homogeneously, provided that the appropriate conditions for its optimal growth are established [14] - [16].

In the literature review conducted, more experimental studies [7] - [10], [12], [15], [17] - [20], for both fabrication and characterization of CSNWs, were found than theoretical ones [21] - [28]. Among these studies, works on CSNWs with circular cross-section predominate [24] - [28], largely due to the difficulties in solving the Schrödinger equation for cross-sections that do not present circular symmetries. Among the theoretical works reported for the latter symmetries are the study of the behavior of a hydrogenoid donor under the effects of electric and magnetic fields [26] and under the effect of fields induced by high frequency lasers [27]. Theoretical investigations of CSNWs with non-circular cross sections include studies of the behavior of single and multi-electron systems with emphasis on the conductance [21], optical [2], electronic [22] properties and the effect of the energy gaps of the materials on the electronic probability density of the systems [23].

It is noteworthy that CSNWs with non-circular cross section are ideal candidates for the creation of quantum rings (QRs) with high degree of resemblance to geometrically perfect structures, which makes them the most appropriate structures for the observation of quantum topological effects such as (ABO) [29].

The aforementioned morphological feature is one of the reasons why CSNWs have been suggested for the construction of artificial molecules. Currently, arrays of coupled QDs are the most commonly used nanostructures to achieve artificial atom conformations; however, an artificial arrangement presenting molecular electronic structure can be obtained with inhomogeneous QRs, where variations in cross-sectional size or radius of curvature along the structure result in potential wells located in small regions [29] - [31]. CSNWs are ideal candidates for this type of structures due to the low diffusion of material in their

heterojunction, since it allows obtaining configurations with high similarity to geometrical structures with high symmetry, as is the case of regular polygons. In particular, the synthesis of GaAs-core CSNWs is a good candidate for the elaboration of artificial benzene molecules due to their regular hexagon morphology [31].

In this work we seek to contribute to the understanding of the properties of mono-electronic systems formed by semiconductor CSNWs, specifically those with hexagonal cross section. This contribution corresponds to the calculation of the energy spectrum and electron density of a conduction electron confined in a CSNW of hexagonal cross section with GaAs core and InAs shell under the effect of a magnetic field applied in the longitudinal direction of the NW, which allows the observation of (ABO), in the framework of the effective mass approximation.

Model and Simulation Details

The study of nanostructured systems by means of models with idealized (circular) symmetry allows to reach a certain understanding of them. However, the morphological characterization of such systems, thanks to instruments such as scanning electron microscopes, has revealed different geometries that diverge from the ideal ones [16] – [32]. The analytical solution of the equations describing systems with non-idealized geometries is a very difficult challenge to solve, therefore, it is important to consider alternative methods for the study of non-ideal geometries, such as the solution of the equations by means of the finite element method.

From the experimental point of view, the fabrication of NWs from materials with Wurtzite and Zinc Blende crystal structures, typical of binary semiconductor compounds, usually results in NWs with hexagonal cross section when fabricated by vapor deposition techniques [16]. Given the importance of this type of semiconductors in NW production [9], [15], [19], in this work a CSNW with hexagonal cross section is studied, modeled as shown in Figure 2.

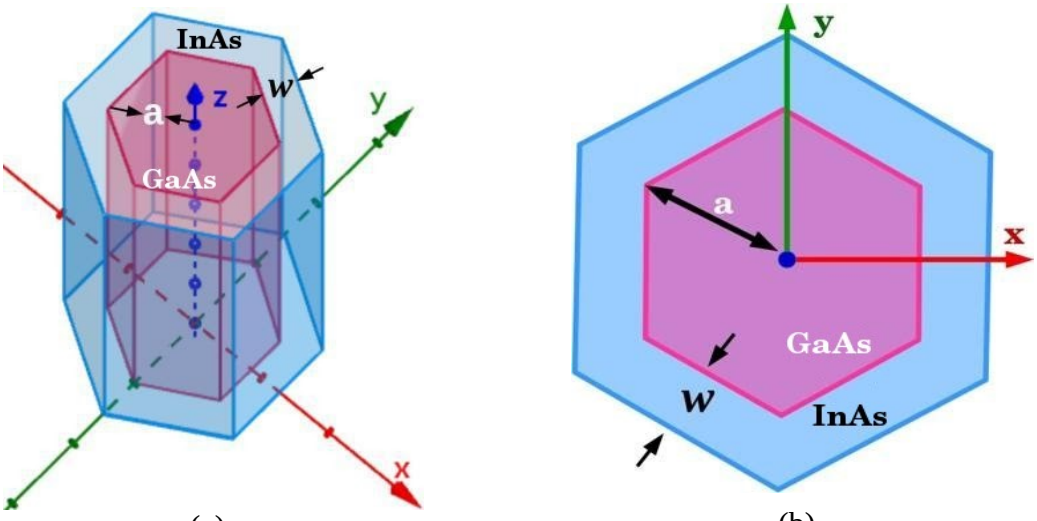

Figure 1. (a) Schematic of the hexagonal cross-section CSNW, with GaAs core and InAs shell (b) Cross section of this system.

For the study of this CSNW, equation (1) was used, which corresponds to the time-independent Schrödinger equation, where B_0 is the magnitude of the magnetic field, $V(\vec{r})$ is the structural confinement potential, different in each of the materials, and with the cyclotron frequency ω_c.

$$\widehat{H}\psi_{xy,n} = E_n\psi_{xy,n} \quad (1)$$

$$\widehat{H} = \frac{-\hbar^2}{2\mathrm{m}^*}\nabla_{xy}^2 + i\hbar\omega_c\left(\chi\partial_y - y\partial_\chi\right) + \frac{(eB_0)^2}{8m^*}(y^2 + x^2) + V(\vec{r}) \quad (2)$$

$$\omega_C = \frac{eB_0}{2m^*} \quad (3)$$

Equation (2) is formulated under the effective mass approximation, the most widely used parameterization in semiconductor physics [33]. This approximation consists of incorporating the effect of the periodic potential of the crystal structure on the apparent mass of the charged particle interacting with the structure. The effective mass is characteristic of each material, since the potential of each crystalline structure is derived from its molecular composition, for the case of GaAs and InAs we have, respectively, values of 0.065 and 0.026 times the mass of the free electron [34].

Dirichlet conditions were imposed at the outer boundary of the structure. The reference confinement potential is that of InAs, with respect to which that of GaAs has a value of 0.697 eV. The potential outside the structure was assumed to be infinite because the structure is considered to be surrounded by air. The core radius, taken as the distance from the center to any of its six vertices, is fixed at 50 nm, while the shell thickness w takes values between 1 and 15 nm.

An important experimental aspect is the ratio between the length of the CSNW and the radius of its cross section, which is usually of the order of 1000 [8], [19], [35], so that the structural confinement in the longitudinal direction is not comparable with that of the cross section. The ratio of 1000 to one between the length of a CSNW and its radius allows to consider only the CSNW cross section as the one responsible for the quantum confinement, since the electron spectrum in a structure with lengths of tens or even hundreds of microns can be considered continuous.

To solve equation (1), the two-dimensional finite element method was used, implemented with COMSOL multiphysics®, with triangular elements and an inhomogeneous and controlled meshing for which the sides of each element were in the range between 0.0131 and 4 nm, and the resolution of the narrow regions was 7 elements.

Results and Discussion

In the following, we discuss the results of the solution of equation (1), which represents the electron quantum-mechanical behavior in the transverse region of the hexagonal CSNW under the effective mass approximation. The results include the analysis of the effects of shell thickness and of the application of a magnetic field in the longitudinal direction of the NW on the electronic probability density, the energy spectrum and the ABOs.

Effect of shell thickness

The possibility of fabricating NWs surrounded by a shell, which thickness can be controlled during the growth process [35], [15], is one of the most interesting features of CSNWs, mainly because the thickness of the shell determines some of their properties, as a consequence of known quantum phenomena occurring at small scale. In the cross section of a CSNW the shell can be considered as a quantum ring surrounding the core. In this work, the shell corresponds to a hexagonal ring with uniform width w.

Figure 2 shows the dependence of the CSNW ground state energy on the thickness of the shell w. It can be seen how, as w decreases, the ground state energy increases markedly and for a valuew = 2.4 nm it remains approximately constant. This behavior is due to the configuration of the structural confinement potential, in which the shell acts as a well which bottom is 697 meV below the ground level.

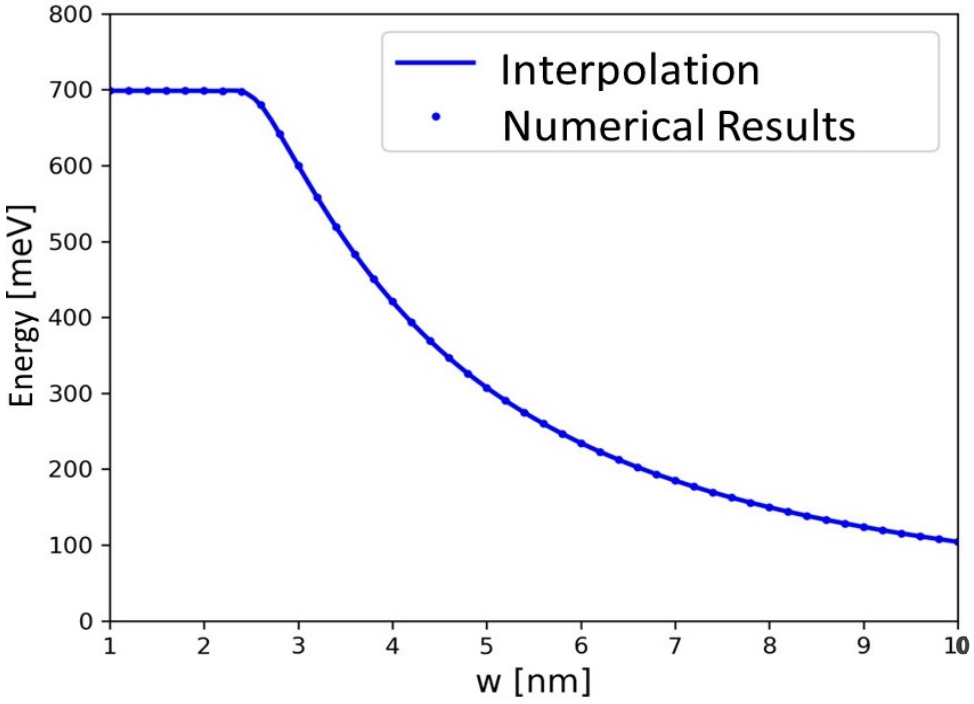

Figure 2. Dependence of the base state energy on the thickness w of the shell.

The threshold value of the shell

Figure 2 shows, that when the thickness of the shell is reduced to a value of about $w = 2.4\ nm$ the minimum thickness that allows, at least one localized state in the shell is reached. We have called this value the threshold value, because it indicates the minimum thickness that the shell can have before the electronic wave function overflows, from the shell to the core and is therefore related to a change from quantum ring to dot regime. This behavior is evidenced in Figure 3. For values of w greater than the threshold value, Figure 3(a), the electron is confined in the shell. For w values close to the threshold value, the electron presents a certain probability of being in the core, Figure 3(b), while for w values much lower than the threshold value, Figure 3(c), it can be seen how the electron is completely located in the core.

When the electron is confined in the core ($w < 2.4\ nm$, see Figure 3(c)), the ground state energy (698 meV) is slightly higher than the confining potential in GaAs (697 meV). For the opposite case, and with a thickness significantly larger than the threshold thickness, it is observed that the highest electronic probability density is found at the six corners of the shell, Figure 3(a). The hexagonal geometry of the shell means that, in the straight segments that form the sides of the hexagon, the confining potential due to the curvature is zero, while at the vertices, which can be considered as pointy corners because the curvature becomes infinite, the potential takes the form of true potential wells [30]. For this reason, the electronic probability distribution of the ground state shows maxima at these vertices. For values of w close to 2.4 nm, in the so-called transition zone, tunneling is observed towards the central region, Figure 3(b), in addition to a change in electronic localization, which moves from the vertices to the straight regions between them; this change in confinement can be attributed to the repulsive effect of the Dirichlet conditions imposed on the boundary, which for thicker shell ($w >> 2.4\ nm$) play a less noticeable role.

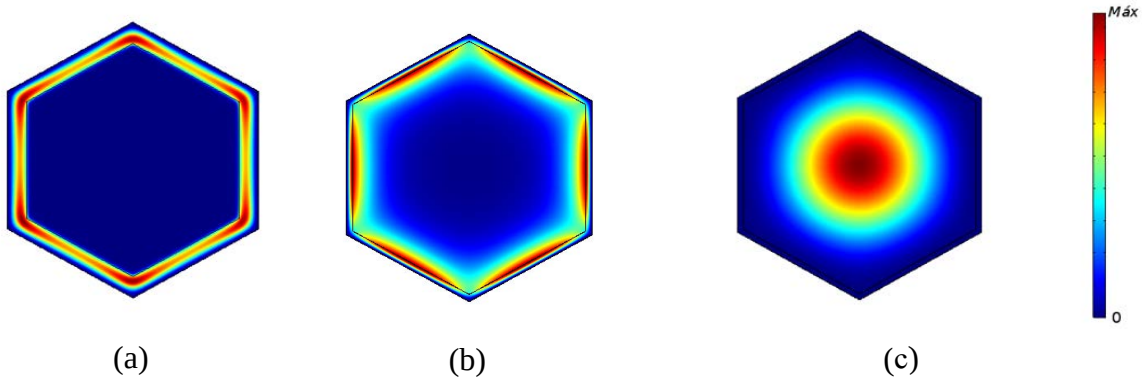

Figure 3. Ground state electron probability densities for CSNW with different shell thickness (a) 8 nm, (b) 2.5 nm and (c) 2 nm.

The confinement at the vertices, for w = 2.4 nm, can be considered as an attractive effect of the vertices. The electron probability density observed when such an attractive effect is present has a regular hexagonal geometry similar to that observed in benzene (C_6H_6) [36].

Energy and electron density for shell greater than the threshold value.

Although the limiting value of w has been taken as 2.4 nm, it is for values of w >7.0 nm that the electron density obtained for CSNW resembles that of the benzene molecule, Figure 4(a). For w values between 2.4 and 7.0 nm the energy level structure of CSNW, Figure 4(b), although similar to that of benzene, does not completely match.

In Figure 4(a) a comparison can be made between the 4 lowest energy states (52.4 to 56.68 meV) and their probability densities obtained with those for benzene [36], since agreement is observed with the bonding and anti-bonding states observed in that molecule, and agreement is also found in the degeneracy of these.

The four higher levels (58.72 to 72.35 meV) present the same degeneracy pattern, and increase of nodes along the shell, expected due to the energetic increase. Levels 4 and 5 of this graph present similarities, both present 3 nodal axes, and it could be thought that they should be part of a single degenerate level, however level 4 requires less energy, since its maxima are located at the vertices of the structure, where there are attractive regions produced by the change of curvature [30], while level 5 requires more energy, since its maxima are located in the straight regions of the shell.

Energy and electron density for shell around the threshold value

Figures 4 (b) and (c) show the eight lowest energy states for a hexagonal CSNW configuration with shell thickness w = 2.5 and 2.45 nm. In contrast to what is observed for shells with w >7.0 nm, Figure 4(c) shows that the ground state does not exhibit vertex confinement. The first five energy levels show the same degeneracy as in the previous case, but at different energies. Beyond the fifth energy level, for w = 2.5 nm and at an energy of 699.50 meV, the degeneracy of the levels is different than for 15 nm shell.

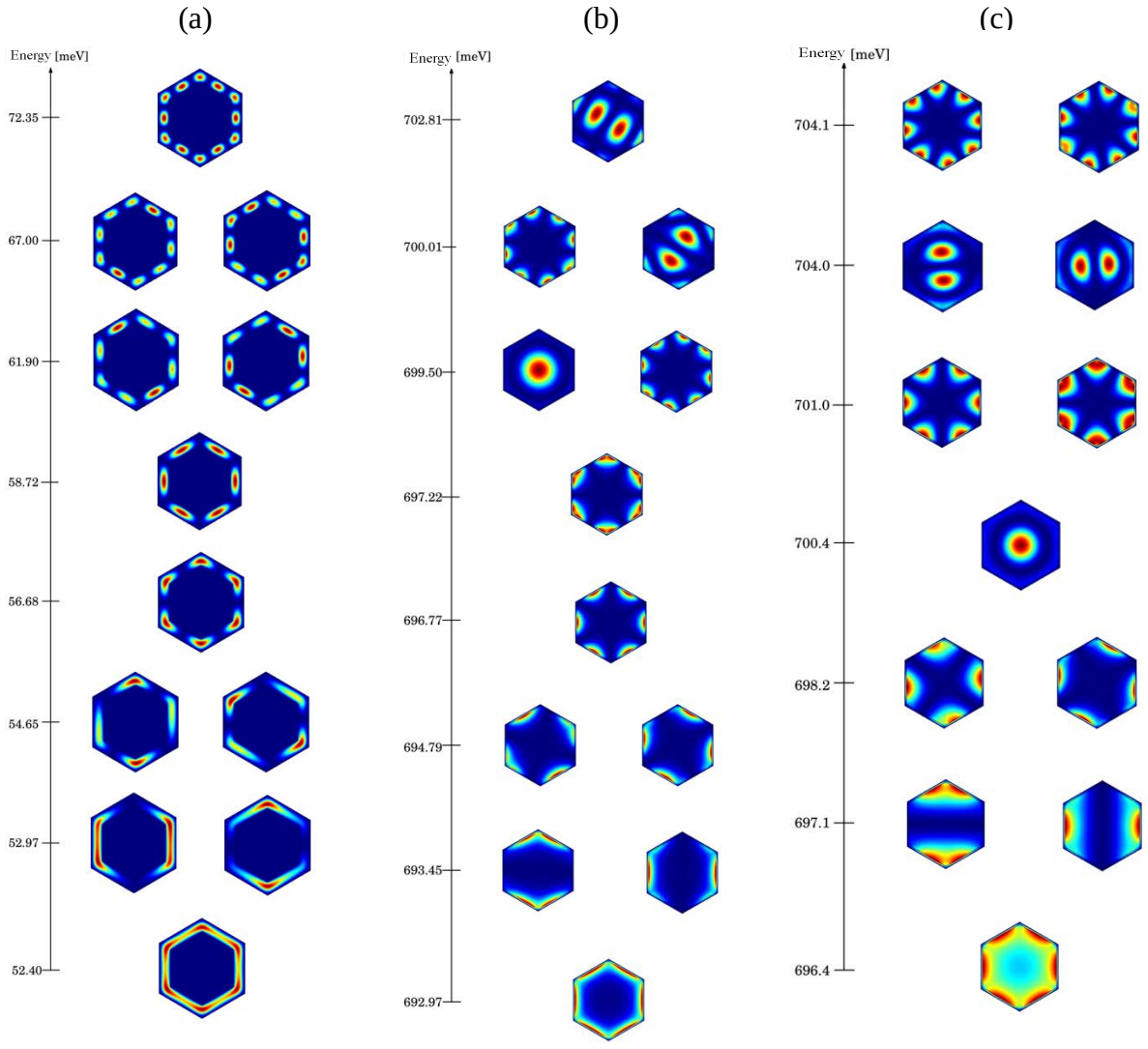

Figure 4. Energy and electron probability densities for shell with width of (a) w=15 nm, (b) w=2.5 nm and (c) w=2.45 nm**.**

Figure 4(c) shows, for the three lower levels, similarity with the cases for w = 15 nm and 2.5 nm, however the upper levels, 4 to 7, do not show agreement. At level 4, an infiltrated state is observed with a higher probability in the central region of the structure, and a degenerate level, 6, in a similar situation. These two levels, which in the case of Figure 4(b) were at levels 6 and 8 respectively, have decreased with decreasing shell thickness.

This difference in probability and de-generations densities may be associated with boundary conditions, the effect of which is more noticeable with small shell thickness and is more appreciable in regions near the corners. The reorganization of levels presented by the system due to the thickness of the shell can be seen in Figure 5.

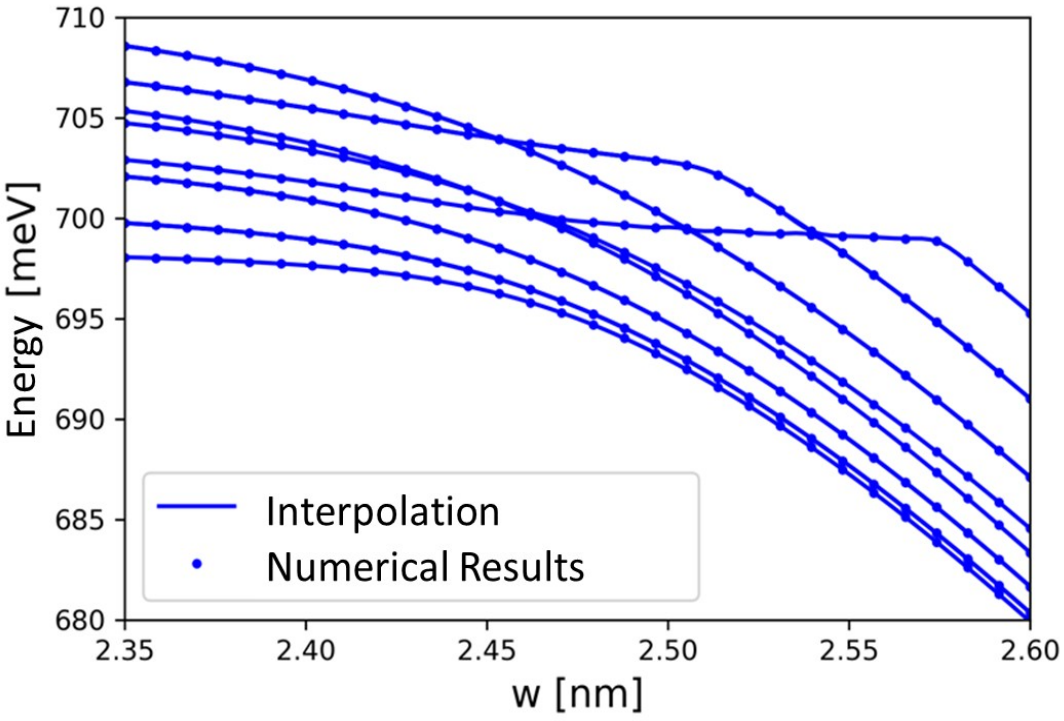

Figure 5. Electron energy in a CSNW with hexagonal cross section and thickness w of the shell.

Figure 5 should be analyzed in a right-left direction. On the far right are 8 levels, which are maintained for shell widths greater than that presented in the figure, and which can be seen in Figure 4. The lower three levels remain unperturbed, as can be seen in the three electron density plots in Figure 4. Each intersection of the graph represents a breakup of the degenerate states and reorganization of them; moving from the right to the left, an intersection is found between levels 7 and 8, this results in the degeneracy of level 8; further to the left, it is observed that the same happens with levels 6 and 7, the latter becoming degenerate again, and leaving level 6 non-degenerate, these two effects can be seen in Figure 4(b). Between 2.50 and 2.45 nm there is a crossover between levels 4, 5 and 6, the consequences of this can be seen in Figure 4(c), and the decrease in the energy spectrum of level 4 is observed, which is very similar to that which in Figure 4(b) corresponds to level 6.

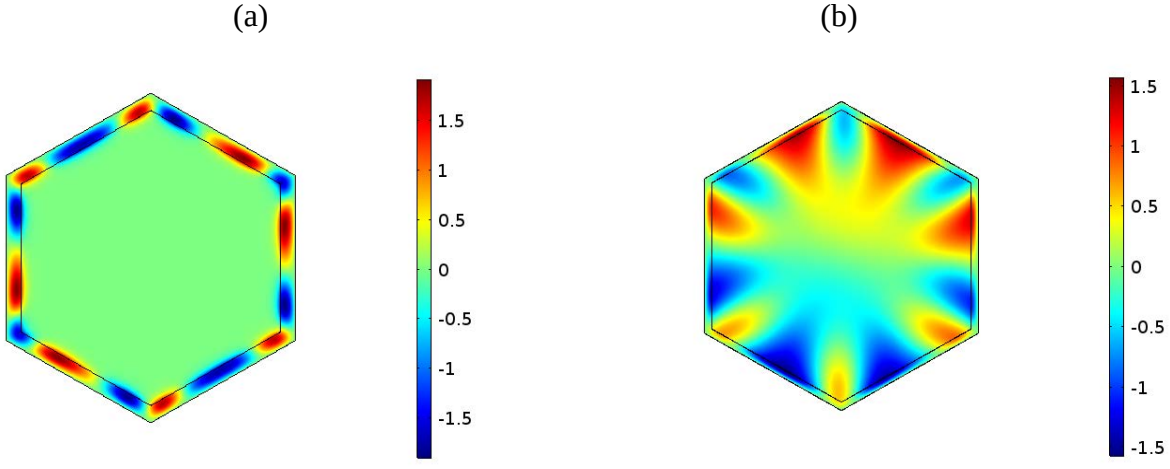

Figure 6. Base state wave functions for CSNW subjected to a magnetic field of magnitude 5 T and shell thickness of (a) 5.0 nm and (b) 2.5 nm.

Effect of the magnetic field

When exposing the CSNW to an external magnetic field perpendicular to the cross section of the nanostructure, an interaction between the electron and this field arises. For shell thicknesses greater than the threshold value, upon application of the magnetic field a change in the electron probability density at the vertices of the hexagon was observed, Figure 6(a), suggesting that the magnetic interaction alters the confinement effect of the shell described in the previous section.

The effect of the magnetic field can be observed as a distortion of the base state wave function, which has six maxima, one at each vertex for w greater than the limiting value. Unlike the six lobes observed in the absence of the magnetic field, Figure 3(a), when the field is present a larger number of these are observed, Figure 6(a). This behavior is also present for shell widths close to the threshold value, Figure 6(b). In Figure 6(b), the radial confinement effect imposed by the diamagnetic term in equation (1) is also observed, in addition to the tunneling to the central region of the structure.

Figure 7 shows the energy spectrum dependence on the intensity of the applied magnetic field. In this spectrum one can clearly appreciate the breakup of the degenerate levels due to the interaction of the electron with the magnetic field, in addition to the ABOs and how these oscillations are affected by the geometry of the system. Unlike what is observed in a circular QR [37] in ABOs no crossover between all energy levels is observed, instead the grouping in subbands of six oscillating energy levels is observed; this grouping in six bands can be attributed to the hexagonal structure. Such ABOs present a period $T = \Delta B = h/e\pi R^2$, where R is the geometric mean radius of the structure, which was calculated by taking into account both the radius of a regular polygon and the apothem.

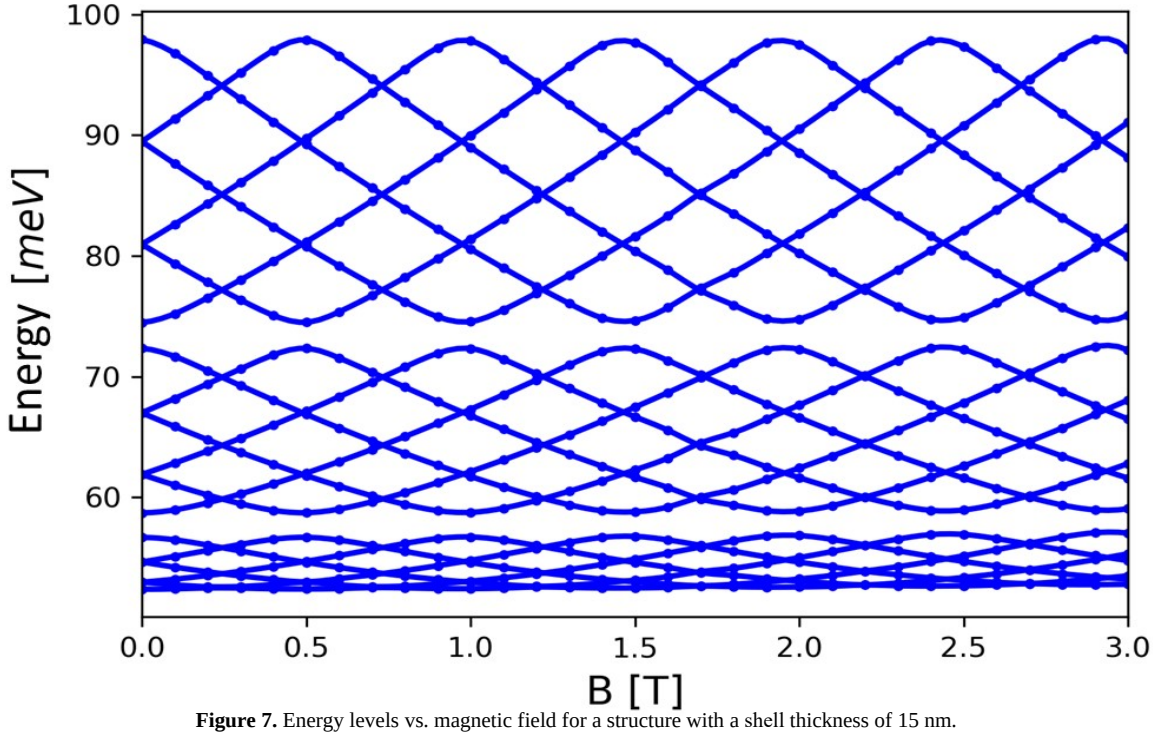

Figure 7. Energy levels vs. magnetic field for a structure with a shell thickness of 15 nm.

Conclusions

The electronic localization effects due to the presence of a shell in nanowires with core-shell structure in the presence of external fields were studied. The effects were studied in the effective mass approximation by means of the solution of the Schrödinger equation with the finite element method. The results obtained show, on the one hand, the capability of the finite element method for the solution of partial differential equations in complex geometries and, on the other hand, the use of such numerical solutions to study physical phenomena of complex nanostructures. In addition, modeling the shell as a structure with a finite barrier potential made it possible to demonstrate the modification suffered by the energy spectrum of the

system due to tunneling and quantum overflow of the wave function towards the core, especially when there are strong magnetic confinement conditions.

It should be noted that one of the most interesting results obtained in the study was the similarity of the electronic probability densities for shell widths greater than 7 nm with those of the benzene molecule. The similarities found suggest that these structures are possible candidates for building artificial molecular systems with great potential for future optoelectronic applications.

Acknowledgments

We are grateful to the Universidad Industrial de Santander (UIS), which through the Vicerrectoría de Investigación y Extensión (VIE), DIEF de Ciencias, financed this research through project 2421.

References

[1] C. Thelander, P. Agarwal, S. Brongersma, J. Emery, L. F. Feiner, A. Forchel, M. Scheffler, W. Riess, B. Ohlsson, U. Gösele et al., "Nanowire-based one-dimensional electronics", *Materials today*, vol. 9, no. 10, pp. 28–35, 2006.

[2] Z. Wang and B. Nabet, "Nanowire optoelectronics", *Nanophotonics*, vol. 4, no. 1, pp. 491–502, 2015.

[3] K. Pathakoti, M. Manubolu, and H.-M. Hwang, "Nanostructures: Current uses and future applications in food science", *Journal of food and drug analysis*, vol. 25, no. 2, pp. 245–253, 2017.

[4] S. S. Bhinder and P. Dadra, "Application of nanostructures and new nano particles as advanced biomaterials", *Asian Journal of Chemistry*, vol. 21, pp. S167, 2009.

[5] J. Esper, P. V. Panetta, M. Ryschkewitsch, W. Wiscombe, and S. Neeck, "Nasa-gsfc nano-satellite technology for earth science missions", *Acta Astronautica*, vol. 46, no. 2-6, pp. 287–296, 2000.

[6] J. Wallentin, N. Anttu, D. Asoli, M. Human, I. Åberg, M. H. Magnusson, G. Siefer, P. Fuss-Kailuweit, F. Dimroth, B. Witzig-mann et al., "InP nanowire array solar cells achieving 13.8 % efficiency by exceeding the ray optics limit", *Science*, vol. 339 (6123), pp. 1057-1060, 2013.

[7] M. Currie, Z. Wang, P. Dianat, P. Prete, I. Miccoli, N. Lo-vergine, and B. Nabet, "Large light emission enhancement in GaAs/AlGaAs coreshell nanowires", *International Conference on One-Dimensional Nanomaterials*, ICON2013, Annecy, France, 2013.

[8] X. Yuan, D. Saxena, P. Caro , F. Wang, M. Lockrey, S. Mokkapati, H. H. Tan, and C. Jagadish, "Strong amplified spontaneous emission from high quality GaAs1–x/Sbx single quantum well nanowires", *The Journal of Physical Chemistry C*, vol. 121, no. 15, pp. 8636–8644, 2017.

[9] N. Sköld, L. S. Karlsson, M. W. Larsson, M. E. Pistol, W. Seifert, J. Trägårdh, and L. Samuelson, "Growth and optical properties of strained GaAs-GaxIn1-xP core- shell nanowires", *Nano letters*, vol. 5, no. 10, pp. 1943–1947, 2005.

[10] J. Richters, T. Voss, D. Kim, R. Scholz, and M. Zacharias, "Enhanced surface-excitonic emission in ZnO/Al2O3 core–shell nanowires", *Nanotechnology*, vol. 19, no. 30, pp. 305202, 2008.

[11] L.-F. Cui, R. Ru o, C. K. Chan, H. Peng, and Y. Cui, "Crystalline-amorphous core- shell silicon nanowires for high capacity and high current battery electrodes", *Nano letters*, vol. 9, no. 1, pp. 491–495, 2008.

[12] S. Furthmeier, F. Dirnberger, M. Gmitra, A. Bayer, M. Forsch, J. Hubmann, C. Schüller, E. Reiger, J. Fabian, T. Korn et al., "Enhanced spin–orbit coupling in core/shell nanowires", *Nature*

communications, vol. 7, pp. 12413, 2016.

[13] M. Hu, K. P. Giapis, J. V. Goicochea, X. Zhang, and D. Poulikakos, "Significant reduction of thermal conductivity in Si/Ge core-shell nanowires", *Nano letters*, vol. 11, no. 2, pp. 618–623, 2010.

[14] M. Tchernycheva, L. Travers, G. Patriarche, F. Glas, J. C. Hamand, G. E. Cirlin, and V. G. Dubrovskii, "Au-assisted molecular beam epitaxy of InAs nanowires: Growth and theoretical analysis", *Journal of Applied Physics*, vol. 102, no. 9, pp. 094313, 2007.

[15] T. Rieger, M. Luysberg, T. Schäpers, D. Grützmacher, and M.-I. Lepsa, "Molecular beam epitaxy growth of GaAs/InAs core– shell nanowires and fabrication of inas nanotubes", *Nano letters*, vol. 12, no. 11, pp. 5559–5564, 2012.

[16] M. Koguchi, H. Kakibayashi, M. Yazawa, K. Hiruma, and T. Katsuyama, "Crystal structure change of GaAs and InAs whiskers from zinc-blende to wurtzite type", *Japanese journal of applied physics*, vol. 31, no. 7R, pp. 20–61, 1992.

[17] L. J. Lauhon, M. S. Gudiksen, D. Wang, and C. M. Lieber, "Epitaxial core–shell and core–multishell nanowire heterostructures", *Nature*, vol. 420, no. 6911, p. 57, 2002.

[18] X. Cartoixà, M. Palummo, H. I. T. Hauge, E. P. Bakkers, and R. Rurali, "Optical emission in hexagonal sige nanowires", *Nano letters*, vol. 17, no. 8, pp. 4753–4758, 2017.

[19] J. A. Czaban, D. A. Thompson, and R. R. LaPierre, "GaAs core- shell nanowires for photovoltaic applications", *Nano letters*, vol. 9, no. 1, pp. 148-154, 2008.

[20] H.-K. Chang and S.-C. Lee, "The growth and radial analysis of Si/Ge core-shell nanowires", *Applied Physics Letters*, vol. 97, no. 25, pp. 251912, 2010.

[21] M. U. Torres, A. Sitek, S. I. Erlingsson, G. Thorgilsson, V. Gudmundsson, and A. Manolescu, "Conductance features of core-shell nanowires determined by their internal geometry", *Physical Review B*, vol. 98, no. 8, pp. 085419, 2018.

[22] B. M. Wong, F. Léonard, Q. Li, and G. T. Wang, "Nanoscale effects on heterojunction electron gases in GaN/AlGaN core/shell nanowires", *Nano letters*, vol. 11, no. 8, pp. 3074–3079, 2011.

[23] N. Luo, G.-Y. Huang, G. Liao, L.-H. Ye, and H. Xu, "Band-inverted gaps in InAs/GaSb and GaSb/InAs core-shell nanowires", *Scientific reports*, vol. 6, p. 38698, 2016.

[24] L. García, I. Mikhailov, and H. Paredes, "Effect of conduction band nonparabolicity on aharonov-bohm oscillations in n-type InAs/GaAs quantum ring", *Journal of Physics: Conference Series*, vol. 935, pp. 12075, 2017.

[25] N. Kleemans, I. Bominaar-Silkens, V. Fomin, V. Gladilin, D. Granados, A. G. Taboada, J. García, P. Offermans, U. Zeitler, P. Christianen et al., "Oscillatory persistent currents in self-assembled quantum rings", *Physical review letters*, vol. 99, no. 14, 2007.

[26] J. Marin, Y. Suaza, and I. Mikhailov, "Hydrogen-like donor in a core-shell nanowire under electric and magnetic fields", *Chemical Physics Letters*, vol. 709, pp. 88–95, 2018.

[27] E. Niculescu and A. Radu, "Laser-induced diamagnetic anisotropy of coaxial nanowires", *Current Applied Physics*, vol. 10, no. 5, pp. 1354-1359, 2010.

[28] S.-K. Kim, R. W. Day, J. F. Cahoon, T. J. Kempa, K.-D. Song, H.- G. Park, and C. M. Lieber, "Tuning light absorption in core/shell silicon nanowire photovoltaic devices through morphological de-sign",

Nano letters, vol. 12, no. 9, pp. 4971–4976, 2012.

[29] P. Corfdir, O. Marquardt, R. B. Lewis, C. Sinito, M. Ramsteiner, A. Trampert, U. Jahn, L. Geelhaar, O. Brandt, and V. M. Fomin, "Excitonic aharonov–bohm oscillations in core–shell nanowires", *Advanced Materials*, vol. 31, no. 3, pp. 1805645, 2019.

[30] E. Switkes, E. L. Russell, and J. L. Skinner, "Kinetic energy and path curvature in bound state systems", *The Journal of Chemical Physics*, vol. 67, no. 7, pp. 3061–3067, 1977.

[31] A. Ballester, J. Planelles, and A. Bertoni, "Multi-particle states of semiconductor hexagonal rings: Artificial benzene", *Journal of Applied Physics*, vol. 112, no. 10, pp. 104317-104317-9, 2012.

[32] P. Yang, H. Yan, S. Mao, R. Russo, J. Johnson, R. Saykally, N. Morris, J. Pham, R. He, and H. J. Choi, "Controlled growth of ZnO nanowires and their optical properties", *Advanced Functional Materials*, vol. 12, no. 5, pp. 323–331, 2002.

[33] M. Burt, "The justification for applying the effective-mass approximation to microstructures", *Journal of Physics: Condensed Matter*, vol. 4, no. 32, pp. 6651-6690, 1992.

[34] I. Vurgaftman, J. á. Meyer, and L. á. Ram-Mohan, "Band parameters for III–V compound semiconductors and their alloys", *Journal of applied physics*, vol. 89, no. 11, pp. 5815–5875, 2001.

[35] F. Haas, K. Sladek, A. Winden, M. Von der Ahe, T. Weirich, T. Rieger, H. Lüth, D. Grützmacher, T. Schäpers, and H. Hardtdegen, "Nanoimprint and selective-area MOVPE for growth of GaAs/InAs core/shell nanowires", *Nanotechnology*, vol. 24, no. 8, pp. 085603, 2013.

[36] R. M. G. Francis A. Carey, "Organic Chemistry", *McGraw Hill*, 2011.

[37] A. Bruno-Alfonso and A. Latgé, "Aharonov-bohm oscillations in a quantum ring: Eccentricity and electric field effects", *Physical Review B*, vol. 71, no. 12, pp. 125312, 2005.